



**HAL**  
open science

## Coupling boundary integral and shell finite element methods to study the fluid structure interactions of a microcapsule in a simple shear flow

Claire Dupont, Anne-Virginie Salsac, Dominique Barthes-Biesel, Marina Vidrascu, Patrick Le Tallec

► **To cite this version:**

Claire Dupont, Anne-Virginie Salsac, Dominique Barthes-Biesel, Marina Vidrascu, Patrick Le Tallec. Coupling boundary integral and shell finite element methods to study the fluid structure interactions of a microcapsule in a simple shear flow. International Conference on Boundary Element and Meshless Techniques (Beteq), Jul 2013, Palaiseau, France. hal-00913201

**HAL Id: hal-00913201**

**<https://inria.hal.science/hal-00913201>**

Submitted on 3 Dec 2013

**HAL** is a multi-disciplinary open access archive for the deposit and dissemination of scientific research documents, whether they are published or not. The documents may come from teaching and research institutions in France or abroad, or from public or private research centers.

L'archive ouverte pluridisciplinaire **HAL**, est destinée au dépôt et à la diffusion de documents scientifiques de niveau recherche, publiés ou non, émanant des établissements d'enseignement et de recherche français ou étrangers, des laboratoires publics ou privés.

# Coupling boundary integral and shell finite element methods to study the fluid structure interactions of a microcapsule in a simple shear flow.

Claire Dupont<sup>1,2</sup>, Anne-Virginie Salsac<sup>2</sup>, Dominique Barthès-Biesel<sup>2</sup>, Marina Vidrascu<sup>3</sup>, Patrick Le Tallec<sup>1</sup>

<sup>1</sup> Laboratoire de Mécanique des Solides (UMR CNRS 7649), Ecole Polytechnique, emails: (dupont, letallec)@lms.polytechnique.fr

<sup>2</sup> Laboratoire de Biomécanique et Bioingénierie (UMR CNRS 7338), Université de Technologie de Compiègne, emails: (a.salsac, dbb)@utc.fr

<sup>3</sup> Equipe-projet REO, INRIA Rocquencourt - LJLL UMR 7958 UPMC, email: marina.vidrascu@inria.fr

**Keywords:** fluid-structure interaction, shell element, finite element method, boundary integral method

**Abstract.** We simulate the motion of an initially spherical capsule in a simple shear flow in order to determine the influence of the bending resistance on the formation of wrinkles on the membrane. The fluid structure interactions are obtained numerically coupling a boundary integral method to solve for the Stokes equation with a nonlinear finite element method for the capsule wall mechanics. The capsule wall is discretized with MITC linear triangular shell finite elements. We find that, at low flow strength, buckling occurs in the central region of the capsule. The number of wrinkles on the membrane decreases with the bending stiffness and, above a critical value, wrinkles no longer form. For thickness to radius ratios below 5%, the bending stiffness does not have any significant effect on the overall capsule motion and deformation. The mean capsule shape is identical whether the wall is modeled as a shell or a two-dimensional membrane, which shows that the dynamics of thin capsules is mainly governed by shear elasticity and membrane effects.

## Introduction

Bioartificial capsules consisting of an internal liquid droplet enclosed by a thin hyperelastic wall have numerous applications in bioengineering and pharmaceuticals, where they are used as vectors for drug targeting or the development of artificial organs. Their membrane may undergo large deformations due to the hydrodynamic stresses exerted by the flows of the internal and suspending fluids. Their motion and deformation are therefore solution of a complex problem of fluid-structure interaction in the viscous flow regime. It is important to predict their behaviour in order to avoid/provoke the membrane rupture depending on the applications.

Different numerical methods have been considered to simulate the dynamics of a capsule in an external flow. Previous studies have solved the membrane equilibrium either locally using spectral elements [1] or bi-cubic B-splines [2], or globally implementing a finite element method [3]. To solve the low Reynolds number equations, the boundary integral method [1,2,3,4] is the technique the most classically used as compared to the lattice Boltzmann method [5] and spectral method [6]. Since the velocity field at any position within the fluid domain is given by surface integrals calculated on the geometric boundaries, it allows reducing the dimension of the problem by one and avoids re-meshing the fluid domain at each time step. It also allows a Lagrangian tracking of the membrane position with high accuracy. The boundary integral – finite element (BI-FE) coupling method, initially proposed by [3], has been shown to be stable in the presence of in-plane compression. It has thus enabled the study of little explored cases, such as the dynamics of a capsule in a pore with a square cross-section [7] or the motion of an ellipsoidal capsule in a simple shear flow, when its revolution axis is initially placed off the shear plane [8].

So far, the capsule wall has typically been considered to be infinitely thin with negligible bending stiffness and modeled as a 2D hyperelastic material. We presently introduce a boundary integral – shell finite element method to take into account the bending stiffness of the capsule wall and study its influence on the motion and deformation of a spherical capsule in an external shear flow. An MITC (mixed interpolation of the tensorial component) shell finite element method is used to model both membrane and bending effects [9]. After a brief outline of the problem at stake, we detail the fluid-structure interaction numerical method and validate it on the classical test of an initially spherical capsule in simple shear flow. We then investigate the influence of the bending resistance on the capsule motion and on the wrinkle formation.

### Problem Statement

We consider an initially spherical microcapsule (radius  $\ell$ ) consisting of a liquid droplet enclosed by a thin membrane. The membrane is a three-dimensional material of thickness  $h$ , shear modulus  $G$ , Poisson coefficient  $\nu$  and bending modulus  $\kappa$ . It is modeled as a midsurface shell defined by the material properties

$$G_s = hG, \quad \nu_s = \nu \quad (1)$$

where  $G_s$  is the surface shear modulus and  $\nu_s$  the surface Poisson coefficient.

The capsule is suspended in a simple shear flow in the  $(\underline{e}_1, \underline{e}_2)$  plane:

$$\underline{v}^\infty = \dot{\gamma} \alpha_2 \underline{e}_1, \quad (2)$$

where  $\dot{\gamma}$  is the shear rate. The inner and outer fluids are supposed to be Newtonian and to have the same viscosity  $\mu$  and density  $\rho$ .

Owing to the small capsule size, the inner and outer flow Reynolds numbers  $\text{Re} = \rho \ell^2 \dot{\gamma} / \mu$  are infinitely small. The dynamics of the microcapsule is mostly governed by the capillary and bending numbers

$$Ca = \frac{\mu \dot{\gamma} \ell}{G_s} \quad \text{and} \quad B = \frac{1}{\ell} \sqrt{\frac{\kappa}{G_s}}. \quad (3)$$

The capillary number compares the viscous to the shear elastic forces and the bending number the bending to the shear elastic forces. The latter can also be considered as the ratio of the membrane thickness  $h$  to the sphere radius  $\ell$ .

### Numerical Method: General Principal

For the first time, the BI-FE method is enriched with shell finite elements to account for the capsule bending stiffness. The capsule wall is discretized with MITC (Mixed Interpolation Tensorial Components) triangular shell finite elements, the nodes being located on the midsurface. The first step consists in computing the displacement field of the capsule membrane material points, as well as the Green-Lagrange strain tensor. The tension tensor is obtained assuming the capsule to follow the Hooke's law. The membrane equilibrium equation, expressed in its weak form, is solved using a finite element method to deduce the viscous load on the membrane. The velocity of the membrane nodes is then obtained solving the Stokes equations in the internal and external fluids with a boundary integral formulation. The new position of the capsule membrane points is finally calculated integrating the velocity with an explicit Euler integration scheme.

### Membrane Mechanics

In this subsection, we briefly describe the shell kinematics based on [9] and [10] as well as the mechanical problem solved. The surface tensor components will be designed with Greek indices and the 3D tensor components with Latin indices. We adopt the Einstein summation convention on repeated indices.

The capsule wall is represented as a shell of midsurface  $S$  and thickness  $h$ . At each instant of time, the midsurface is defined by the 2D chart  $\varphi(\xi^1, \xi^2)$ , which takes values in the bounded open subset  $\omega \in \mathbb{R}^2$ . It is convenient to define the local covariant base  $(\underline{a}_1, \underline{a}_2, \underline{a}_3)$  following the midsurface deformation. The two base vectors  $(\underline{a}_1, \underline{a}_2)$  are tangent to the midsurface

$$\underline{a}_\alpha = \varphi_{,\alpha}, \quad \alpha = 1, 2 \quad (4)$$

where the notation  $_{,\alpha}$  denotes the partial derivative with respect to  $\xi^\alpha$ . The third vector  $\underline{a}_3$  is the unit normal vector  $\underline{n}$  of the capsule midsurface  $S$ . The contravariant base  $(\underline{a}^1, \underline{a}^2, \underline{a}^3)$  is defined by  $\underline{a}^\alpha \cdot \underline{a}_\beta = \delta_\beta^\alpha$ , with  $\delta_\beta^\alpha$  the Kronecker tensor and  $\underline{a}^3 = \underline{a}_3 = \underline{n}$ . The three-dimensional position within the capsule wall is given by

$$\underline{\varphi}^{3D}(\xi^1, \xi^2, \xi^3) = \underline{\varphi}(\xi^1, \xi^2) + \xi^3 \underline{a}_3(\xi^1, \xi^2), \quad (5)$$

for  $(\xi^1, \xi^2, \xi^3)$  in the reference domain

$$\omega^{3D} = \left\{ (\xi^1, \xi^2, \xi^3) \in \mathbb{R}^3 / (\xi^1, \xi^2) \in \omega, \xi^3 \in \left[ -\frac{h(\xi^1, \xi^2)}{2}, \frac{h(\xi^1, \xi^2)}{2} \right] \right\}. \quad (6)$$

We define the 3D covariant base vector  $(\underline{g}_1, \underline{g}_2, \underline{g}_3)$  such that

$$\underline{g}_\alpha = \varphi_{,\alpha}^{3D} = \underline{a}_\alpha + \xi^3 \underline{a}_{,\alpha} \quad \text{and} \quad \underline{g}_3 = \underline{a}_3. \quad (7)$$

The 3D contravariant base  $(\underline{g}^1, \underline{g}^2, \underline{g}^3)$  is likewise defined by  $\underline{g}^m \cdot \underline{g}_n = \delta_n^m$ . The components of the 3D metrics tensor are

$$g_{\alpha\beta} = \underline{g}_\alpha \cdot \underline{g}_\beta, \quad g_{\alpha 3} = 0, \quad \text{and} \quad g_{33} = 1. \quad (8)$$

We assume that the displacement satisfies the Reissner-Mindlin kinematical assumption, i.e. the material line orthogonal to the midsurface remains straight and unstretched during deformation. The displacement is then expressed by

$$\underline{u}^{3D}(\xi^1, \xi^2, \xi^3) = \underline{u}(\xi^1, \xi^2) + \xi^3 \underline{\theta}_\lambda(\xi^1, \xi^2) \underline{a}^\lambda(\xi^1, \xi^2).$$

The first term  $\underline{u}$  represents the global infinitesimal displacement of a line perpendicular to the midsurface at the coordinates  $(\xi^1, \xi^2)$ . The second term is the displacement due to the rotation of this line.

The deformation of the membrane is computed from the displacement. The expression of the nonlinear 3D Green-Lagrange strain tensor is

$$e_{ij} = \frac{1}{2} \left( \underline{g}_i \cdot \underline{u}_j^{3D} + \underline{g}_j \cdot \underline{u}_i^{3D} + \underline{u}_i^{3D} \cdot \underline{u}_j^{3D} \right) \quad i, j = 1, 2, 3. \quad (10)$$

The second Piola-Kirchhoff tension tensor  $\underline{\underline{\Sigma}}$  is then obtained from

$$\underline{\underline{\Sigma}} = \frac{\partial w(\underline{u}^{3D})}{\partial \underline{\underline{e}}}, \quad (11)$$

where the strain energy function takes the form

$$w(\underline{u}^{3D}) = \frac{1}{2} \int_{\omega^{3D}} [C^{\alpha\beta\lambda\mu} e_{\alpha\beta}(\underline{u}^{3D}) e_{\lambda\mu}(\underline{u}^{3D}) + D^{\alpha\lambda} e_{\alpha 3}(\underline{u}^{3D}) e_{\lambda 3}(\underline{u}^{3D})] d\omega \quad \alpha, \beta, \lambda, \mu = 1, 2. \quad (12)$$

with

$$C^{\alpha\beta\lambda\mu} = G_s \left( g^{\alpha\beta} g^{\lambda\mu} + g^{\alpha\mu} g^{\beta\lambda} + \frac{2\nu_s}{1-\nu_s} g^{\alpha\beta} g^{\lambda\mu} \right), \quad (13)$$

$$D^{\alpha\lambda} = 4G_s g^{\alpha\lambda} \quad (14)$$

for the Hooke's law. Tensions, which are forces per unit length of the deformed midsurface, are obtained integrating the stresses across the wall thickness.

Knowing the internal tension tensor, the unknown viscous load exerted by the fluid on the membrane can be calculated solving the wall equilibrium

$$\nabla_s \cdot \underline{\underline{T}} + \underline{q} = 0. \quad (15)$$

The operator  $\nabla_s$  is the surface gradient and  $\underline{\underline{T}}$  the Cauchy tension tensor such that

$$\underline{\underline{T}} = \frac{1}{J} \underline{\underline{F}} \cdot \underline{\underline{\Sigma}} \cdot \underline{\underline{F}}^T \quad (16)$$

with  $J$  the Jacobian and  $\underline{\underline{F}}$  the deformation gradient with respect to the reference configuration.

The local equilibrium (eq. (15)) is then written in a weak form using the virtual work principle and solved by means of the finite element method. Let  $V$  be the Sobolev space  $H^1$ . For any virtual displacement field  $\hat{\underline{u}}^{3D} \in V$ , the internal and external virtual work balance requires

$$\int_{\omega^{3D}} \hat{\underline{u}}^{3D} \cdot \underline{q} d\omega = \int_{\omega^{3D}} \underline{\underline{\Sigma}} : \underline{\underline{\delta\hat{e}}} d\omega \quad (17)$$

where  $\underline{\underline{\delta\hat{e}}} = \underline{\underline{e}}(\underline{U}^{3D} + \hat{\underline{u}}^{3D}) - \underline{\underline{e}}(\underline{U}^{3D})$  with  $\underline{U}^{3D}$  the displacement in the reference configuration. The equation is solved to compute the viscous load  $\underline{q}$ .

### Internal and External Flow Dynamics

Knowing the load  $\underline{q}$ , the velocity of the points can be expressed as an integral equation over the deformed capsule surface  $S$  using the boundary integral method:

$$\forall \underline{\varphi}_0^{3D} \in \omega^{3D}, \quad \underline{v}(\underline{\varphi}_0^{3D}) = \underline{v}^\infty(\underline{\varphi}_0^{3D}) - \frac{1}{8\pi\mu} \int_S \left( \frac{\underline{I}}{\|\underline{r}\|} + \frac{\underline{r} \otimes \underline{r}}{\|\underline{r}\|^3} \right) \cdot \underline{q}(\underline{\varphi}'^{3D}) dS(\underline{\varphi}'^{3D}), \quad (18)$$

where  $\underline{v}^\infty$  is the undisturbed flow velocity and  $\underline{I}$  is the identity vector. The vector  $\underline{r} = \underline{\varphi}^{3D} - \underline{\varphi}'^{3D}$  is the distance vector between the point  $\underline{\varphi}^{3D}$ , where the velocity vector is calculated, and the point  $\underline{\varphi}'^{3D}$  that describes the midsurface  $S$  in the integral.

The displacement is related to the velocity  $\underline{v}$  of the wall through the kinematic condition:

$$\underline{v}(\xi^1, \xi^2, \xi^3) = \underline{u}_t^{3D}(\xi^1, \xi^2, \xi^3) \quad (19)$$

where  $\cdot_t$  is the time derivative. An explicit Euler method is then used to integrate the velocity over time and obtain the new position of the wall points.

## Discretization

The capsule wall is discretized using linear triangular shell finite elements. We use the mixed interpolation of the tensorial component approach, which can handle the modeling of objects with wall thicknesses much smaller than their characteristic size, a situation that is prone to locking phenomena [9,10,11]. The MITC approach is based on a mixed formulation that interpolates strains and displacements separately and connects both interpolations at specific tying points. In the following, we will show results for MITC3 linear elements consisting of three nodes (one at each vertex) with 5 degrees of freedom by node.

The mesh of the spherical capsule is generated by inscribing an icosahedron (regular polyhedron with 20 triangular faces) in a sphere. The elements are subdivided sequentially until the desired number of elements is reached [3]. We denote  $\eta$  the mesh size.

## Validation

Before coupling the finite element method to the fluid solver, we have validated the mechanical behavior of the shell finite elements in large static deformations by simulating the inflation of a capsule under an internal pressure  $p$ . During the inflation, the wall is subjected to an isotropic traction characterized by the stretch ratio  $\lambda = 1 + \alpha$ . The bending resistance plays no role in this test case. We have plotted the evolution of the pressure  $p$  according to the inflation factor  $\alpha$  (Fig.1). The numerical results are in agreement with the analytic results. The error remains small in all cases. It increases with increasing wall thickness  $h$  and decreasing number of elements. Among the simulated cases, it is therefore maximum when the capsule is modeled with  $B = 0.1$  and 1280 MITC3 elements. Even in this case, it is only equal to 0.49%, which validates the shell finite element method.

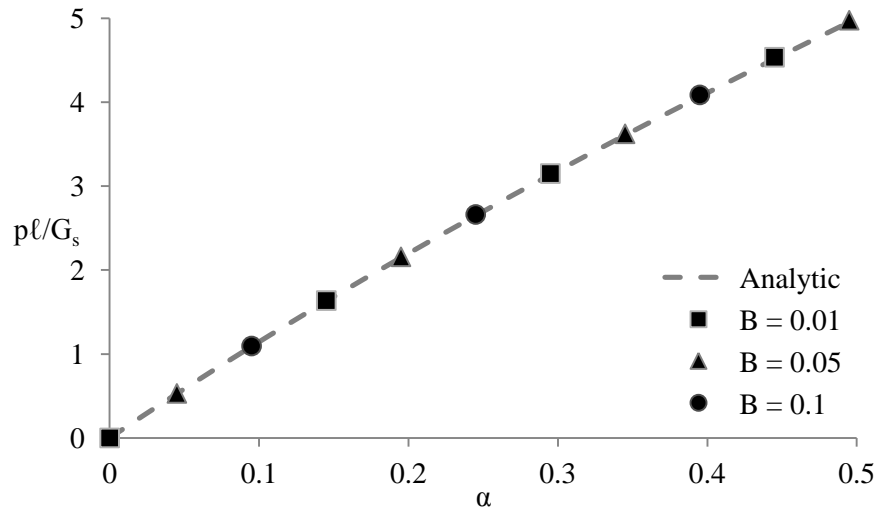


Fig.1: Non-dimensional pressure as a function of the inflation factor  $\alpha$  for bending numbers  $B = 0.01, 0.05$  and  $0.1$ . The capsule wall is discretized with 5120 MITC3 elements.

We have then studied the convergence of the numerical procedure by simulating the motion of an initially spherical capsule in a simple shear flow at  $Ca = 0.6$ . The numerical procedure converges linearly with  $\dot{\gamma}\Delta t$  and quadratically with  $\eta$ . In the following, all the results are provided for 5120 MITC3 elements and a time step  $\dot{\gamma}\Delta t = 10^{-3}$ . The characteristic mesh size is then  $\eta = 5 \times 10^{-2}$ .

## Capsule Dynamics in a Simple Shear Flow

We consider the dynamics of an initially spherical capsule in a simple shear flow at  $Ca = 0.6$ . For all the values of the bending number ( $B \neq 0$ ), the capsule is elongated in the straining direction at the steady state, while the vorticity of the flow induces the rotation of the wall around the steady deformed shape. The larger the capillary number, the more elongated the capsule (Fig. 2). This motion, called *tank-treading*, is exactly the same as that observed when the wall of the capsule is modeled with a membrane model ( $B = 0$ ) [2,3].

The deformed shape can be approximated by its ellipsoid of inertia. We define  $L_1$  and  $L_2$  the lengths of the two principal axes of the ellipsoid of inertia in the shear plane. The deformation of the capsule in the shear plane can be measured by the Taylor parameter  $D_{12}$ :

$$D_{12} = \frac{L_1 - L_2}{L_1 + L_2} \quad (23)$$

To determine the influence of the bending resistance on the average shape in the shear plane, we compare the Taylor parameter at steady state  $D_{12}^\infty$  for several capillary numbers and two values of bending number (Fig. 3). For a given capillary number, the capsule has the same average shape in the shear plane as the one predicted when the capsule wall is modeled as a two-dimensional membrane (without bending resistance).

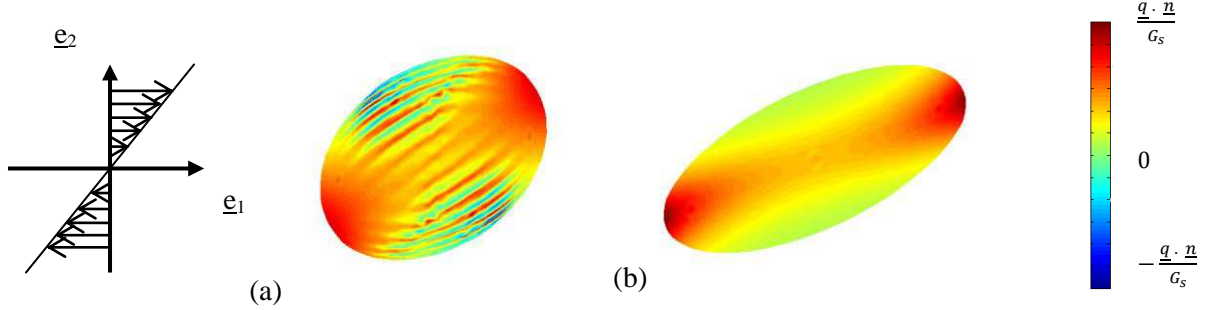


Fig.2: Steady deformed shape for a capsule with  $B = 0.005$  at (a)  $Ca = 0.1$  and (b)  $Ca = 0.6$ . The color scale corresponds to the normal load  $\underline{q} \cdot \underline{n}$ , where the maximum value is equal to  $\underline{q} \cdot \underline{n} / G_s = 0.5$  at  $Ca = 0.1$  and 2.5 at  $Ca = 0.6$ .

When the capsule wall is modeled with a membrane model ( $B = 0$ ), wrinkles appear in the central region of the capsule for capillary numbers below a critical value  $Ca_L$  (Fig. 4a). They result from the presence of compressive tensions in the equatorial area and are in the straining direction. They persist at steady state. Wrinkles are observed at exactly the same location with the shell model (Fig. 4b,c) for low values of  $B$ . When the bending number is increased, the wrinkle wavelength decreases: it is due to the increase in bending stiffness (Fig. 3b,c). For  $B = 0.05$ , the wrinkles no longer form (Fig. 4d). There is therefore a critical bending number, above which the capsule wall is too stiff for buckling to occur.

For capillary numbers above  $Ca_L$ , the capsule is more elongated by the flow (Fig. 2b): the tensions at the equator become positive and the wrinkles disappear.

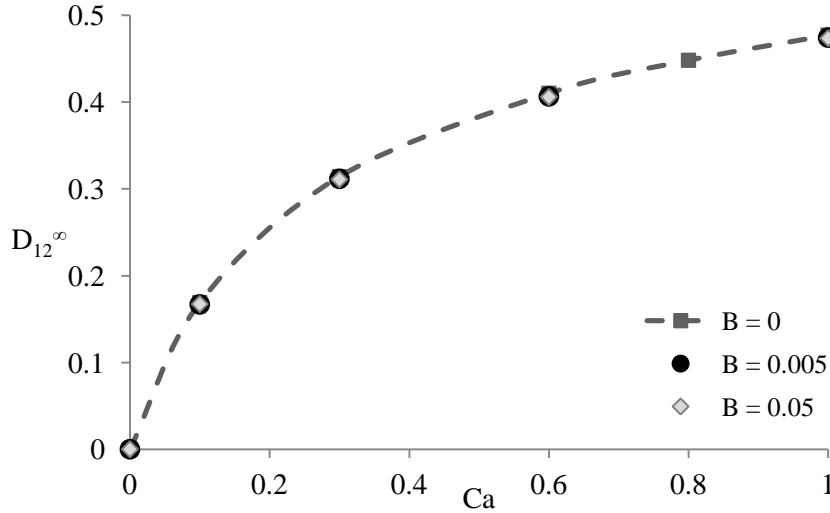


Fig. 3: Values of  $D_{12}^\infty$  as a function of  $Ca$  for bending numbers  $B = 0, 0.005$  and  $0.05$ , for an initially spherical capsule subjected to a simple shear flow.

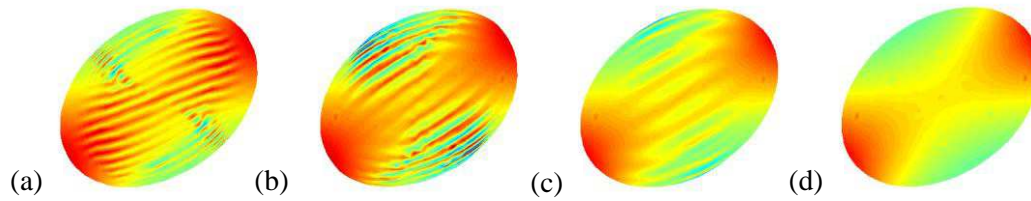


Fig. 4: Steady-state profiles of capsules subjected to a simple shear flow ( $Ca = 0.1$ ): bending number  $B = 0$  (membrane model) (a),  $B = 0.005$  (b),  $B = 0.01$  (c) and  $B = 0.05$  (d). The color scale is the same as in as Fig.2. The maximum value is equal to  $\underline{q} \cdot \underline{n} / G_s = 0.5$ .

## Conclusion

We have simulated the motion of a capsule in a simple shear flow using a boundary integral - MITC shell finite element coupling strategy. The numerical method is stable and free of locking phenomenon. We have shown that the motion and deformation of a thin membrane capsule is marginally influenced by the bending stiffness. The latter controls the amplitude and wavelength of the wrinkles that appear at low capillary number in the straining direction. However, the average deformed shape that the capsule assumes, as it tank-treads, remains identical to that predicted by a two-dimensional membrane model.

## References

- [1] W. R. Dodson, P. Dimitrakopoulos *Spindles, cups, and bifurcation for capsules in Stokes flow*. Phys. Rev. Lett., **101** (20), 208102 (2008).
- [2] É. Lac, D. Barthès-Biesel, N. A. Pelekasis, J. Tsamopoulos *Spherical capsules in three-dimensional unbounded Stokes flow : effect of the membrane constitutive law and onset of buckling*, J. Fluid Mech., **516**, 303–334 (2004).
- [3] J. Walter, A.-V. Salsac, D. Barthès-Biesel, P. Le Tallec *Coupling of finite element and boundary integral methods for a capsule in a Stokes flow*, Int. J. Num. Meth. Engng, **83**, 829–850 (2010).
- [4] C. Pozrikidis *Finite deformation of liquid capsules enclosed by elastic membranes in simple shear flow*, J. Fluid Mech., **297**, 123–152 (1995).
- [5] Y. Sui, H. T. Low, Y. T. Chew, P. Roy *Tank-treading, swinging, and tumbling of liquid-filled elastic capsules in shear flow*. Phys. Rev. E, **77** (1), 016310 (2008).
- [6] S. Kessler, R. Finken, U. Seifert *Swinging and tumbling of elastic capsules in shear flow*. J. Fluid Mech., **605**, 207–226 (2008).
- [7] X.-Q. Hu, A.-V. Salsac, D. Barthès-Biesel *Flow of a spherical capsule in a pore with circular or square cross-section*, J. Fluid Mech., **705**, 176–194 (2012).
- [8] C. Dupont, A.-V. Salsac, D. Barthès-Biesel *Off plane motion of a prolate capsule in shear flow*, J. Fluid Mech., **721**, 180-198 (2013).
- [9] D. Chapelle, K. J. Bathe *The Finite Element Analysis of Shells – Fundamentals*, Computation Fluid and Solid Mechanics. Springer (2003).
- [10] I. Paris Suarez *Robustesse des éléments finis triangulaires de coque*, PhD Thesis, Université Pierre et Marie Curie (Paris VI) (2006).
- [11] P.-S. Lee, K.-J. Bathe *Development of MITC isotropic triangular shell finite elements*, Comp. Struct, **82**, 945–962 (2004).